

# 1385. Influence law of tower stiffness on vertical stiffness of three-tower self-anchored suspension bridge based on frequency formulas

Chao Zhang<sup>1</sup>, Kai Huang<sup>2</sup>

College of Civil Engineering, Fuzhou University, Fuzhou, Fujian, 350108, China

<sup>2</sup>Corresponding author

E-mail: <sup>1</sup>zhangchao1985@fzu.edu.cn, <sup>2</sup>huangkai@fzu.edu.cn

(Received 21 June 2014; received in revised form 22 August 2014; accepted 7 September 2014)

**Abstract.** In this paper, frequencies of low order vertical modals for three-tower self-anchored suspension bridge (TSSB) are studied. The first three-tower self-anchored suspension bridge is taken as prototype in the paper. The finite element model of the bridge is established. And dynamic characteristics are analyzed. Based on Rayleigh method, frequency formulas of 1st asymmetric vertical vibration (AVV) and symmetric vertical vibration (SVV) are deduced considering contribution of towers stiffness. The accuracy of deduced formulas was validated by results of numerical analysis and modal test. Stiffness characteristic difference between TSSB and multi-tower earth-anchored suspension bridge (MESB) is researched based on frequency formulas. The significant difference is gravity stiffness component in frequency formulas. At last, influence law of tower stiffness on vertical frequencies was studied based on validated formulas. The results indicated that: 1) middle tower stiffness and side tower stiffness play important role in frequency of 1st AVV and SVV respectively. Frequencies are enlarging as tower stiffness increasing; 2) when tower stiffness is low, deduced frequency formulas are the same as formulas neglecting influence of tower stiffness in reference paper; 3) based on deduced frequency formulas, expressions of critical tower stiffness for simplified formulas are proposed.

**Keywords:** three-tower self-anchored suspension bridge, frequency formula, tower stiffness, critical stiffness.

## 1. Introduction

Three-tower self-anchored suspension bridge (TSSB) is one new kind of bridge, which combines the advantages of self-anchored suspension bridge and three-tower suspension bridge [1, 2]. TSSB is one of the best kinds of bridge for urban medium-span bridge, which has particular adaptability to site of W shape [3]. It has many advantages [4], such as elegant appearance, good site adaptive capacity and relative larger across ability. Louzhou Bridge is the first TSSB, which is built Fuzhou, China, in 2012 [5]. And this kind of bridge can be built more in any place in the world.

As lacking of effective constraints from cables, equivalent stiffness of middle tower in TSSB is low [6]. Therefore, the static and dynamic mechanical properties of three-tower suspension bridge are quite different from traditional double-tower suspension bridge [7]. Among them, free vibration characteristics is quite different. An experiment of scaled multi-tower suspension bridge specimen has been made to study its dynamic characteristics [8]. Jiao (2010) [9] studied dynamic characteristic of Taizhou Bridge, which is a two-span three-tower earth-anchored suspension bridge (TESB). The studied shows that frequency of 1st vertical vibration is 0.08267 Hz, whose modal shape is asymmetric vibration. Related researches show the 1st vertical vibration is usually shown as asymmetric vertical vibration as equivalent stiffness of middle tower is low [10].

Dynamic characteristics of bridge are the base for earthquake and wind resistant design [11, 12]. At present, finite element method (FEM) is widely used in accurate analyzing vibration frequencies and mode shapes. Jiao (2010) [13] established the finite element model of TSSB by ABAQUS and studied effects of elastic restraints between mid-tower and girders on dynamic property of TESSB. Wang (2014) [14] developed a three-dimensional finite element model to study

the free vibration characteristics of a triple-tower twin-span suspension bridge during the construction phase and right after the erection of the main cable. Wang (2010) [15] studied the dynamic characteristics of the Taizhou Yangtze River Bridge, the first triple-tower long-span suspension bridge in China based on ABAQUS. The results showed the vertical, lateral and torsional stiffness of girder have different effects on the dynamic characteristics of triple-tower suspension bridges. Furthermore, the parametric analysis on the structural flutter stability of Taizhou Yangtze River Bridge was carried out in 2014 [16].

However, there are some disadvantages of FEM, especially on preliminary design phase. For example, it is time-consuming to comparing different design proposals and difficult to reveal influence law of special parameters. In this sense, frequency estimation formulas are fit, as it can quickly provide general frequencies for estimating on preliminary design phase and validating on fine numerical modeling analysis phase [17]. In addition, we can easily get the influence rules of each structure parameter from frequency formulas [18]. Therefore, the frequency formulas are meaningful for quick calculating frequencies. And Chao (2013) [19] deduced frequency formulas of first order vertical modals for TSSB. However, both of them have not considered the effect of tower stiffness on frequencies, which is significant for three-tower suspension bridge in most cases.

In this paper, the frequency estimation formulas of vertical vibration for TSSB considering influence of tower stiffness are deduced by Rayleigh method. Based on deduced formulas, different dynamic mechanical properties between three-tower and double-tower self-anchored suspension bridge are studied based on frequency formulas. And influence law of tower stiffness on vertical frequency is discussed in detail.

## 2. Typical TSSB description and finite element modeling

### 2.1. Description of typical TSSB – Louzhou Bridge

Louzhou Bridge is the first three-tower self-anchored suspension bridge in the world. It is taken as prototype structure of three-tower self-anchored suspension bridge (TSSB) in this paper shown in Fig. 1. This bridge, crossing the Ming River at Fuzhou, China, was opened to traffic in 2012.

The arrangement of the spans along the bridge is 80 m+168 m+168 m+80 m, with an overall length of 496 m. The total width of the bridge deck is 43 m. The suspension bridge system is composed of two sets of suspension cables anchored at the continuous steel deck directly without any anchorage block. Span ratio of main span is 1:6, while that of side span is 1:12.88. The space between slings is 7 m. The deck over the four spans is supported by cables and bearings. Other structural parameters are shown in Table 1.

**Table 1.** Structural parameters of Louzhou Bridge (Unit: m, t, kN)

Parameter	Value	Parameter	Value	Parameter	Value
$f_1$	6.35	$h_t$	50.85	$E_c$	1.95E+08
$f_2$	28.00	$*S_{t1}$	4.33E+04	$E_g$	2.06E+08
$l_1$	80.00	$*S_{t2}$	4.33E+04	$E_t$	3.45E+07
$l_2$	168.00	$M_c$	0.73	$*A_c$	0.0474
$l_{s1}$	103.42	$M_g$	33.40	$A_g$	1.50
$l_{s2}$	207.71	$*M_t$	42.10	$I_g$	1.69

Note: 1)  $f_1$  ( $f_2$ ),  $l_1$  ( $l_2$ ),  $l_{s1}$  ( $l_{s2}$ ) stand for rise, span, equivalent cable length for side span (middle span) respectively; 2) subscript of  $c$ ,  $g$ ,  $t$  indicate cable, girder and tower respectively; 3)  $S$ ,  $M$ ,  $E$ ,  $A$  stand for tower equivalent stiffness, linear mass, elasticity modulus and area respectively; 4) superscript \* means the value for each one.

### 2.2. Finite element modeling

For purposes of this study, a complete 3D FE model was developed in SAP2000N as shown in Fig. 2. This model is used for both static and dynamic analyses. The FE model consists of 1418

nodes and 1664 elements. The bridge towers were represented by three-dimensional multilevel portal frames with the two legs fixed at the base. The soil-structure interaction was not considered in this model.

The geometric properties of three-dimensional beam elements of towers and piers were calculated from design drawings. Since cross sections of tower legs are decreasing from base to top, sectional properties of beam elements for tower were assumed to be uniform section in each 2 m element. Tower equivalent stiffness is  $4.33E+04$  kN/m shown in Table 1.

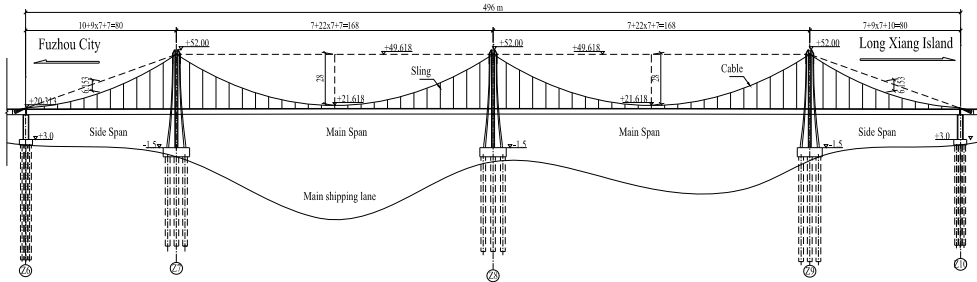


Fig. 1. Elevation figure of Louzhou Bridge (unit: m)

The equivalent beam was connected to the suspenders through a series of horizontal rigid arm members. The bearings between the deck and the towers were represented as swing rigid links so as to allow free longitudinal motion of the deck. The lateral motion of the deck relative to the towers was restricted through horizontal rigid links.



Fig. 2. Louzhou Bridge: a) panorama and b) 3D finite-element model

### 2.3. Modal analysis

Modal analysis is needed to determine the natural frequencies and mode shapes of free vibration. The initial equilibrium configuration is important in suspension bridges since it is a starting position to perform the succeeding analysis [20]. Therefore, the dead load has a significant influence on the stiffness of suspension bridge. In numerical analysis, this influence can be taken into account through the static analysis under the dead load and cable tensions before dynamic analysis is carried out.



Fig. 3. Mode shape of 1st AVV



Fig. 4. Mode shape of 1st SVV

In this paper, modal analysis is carried out based on static analysis under dead loading and cable pre-tensions. We can get the natural frequencies and mode shapes. In general, modal analysis of the Louzhou Bridge showed the modes were arranged in certain sequence: longitudinal mode, vertical modes, lateral modes and torsion modes. As we mainly concern about the vertical stiffness of TSSB, the first 2 vertical modes and frequencies are shown in Fig. 3 and Fig. 4. The frequencies of the 1st AVV and SVV are 0.4481 Hz and 0.6295 Hz respectively. More information of dynamic characteristics is shown in reference [21].

### 3. Frequency formulas for vertical vibration

#### 3.1. Rayleigh method

Rayleigh’s method is a technique for finding natural frequencies by equating the maximum kinetic energy of a system with the maximum potential (often strain) energy. Rayleigh’s method is a widely used, classical method for the calculation of the natural vibration frequency of a structure in the low order. According to Rayleigh’s method, we can get the formula as followed:

$$\omega^2 = \frac{U_{\max}}{T_{\max}} = \frac{\int_0^l EI(x) (\bar{\phi}''(x))^2 dx}{\int_0^l m(x) (\bar{\phi}(x))^2 dx}, \tag{1}$$

where,  $U_{\max}$  stands for maximal value of gravitational potential energy;  $T_{\max}$  stands for maximal value of kinetic energy;  $\bar{\phi}(x)$  is the deformation function of each component;  $\bar{\phi}''(x)$  is the quadratic differential form of  $\bar{\phi}(x)$ .

#### 3.2. Frequency formulas and derivation process

Some parameters are defined for simplified expression during the formulas derivation process, shown as followed.

$l_i$  is the length of girder in the  $i$ th span;  $f_i$  is the rise of cable in the  $i$ th span;  $h_i$  is the height of the  $i$ th tower;  $y_i$  is the geometric alignment of cable in the  $i$ th span, whose expression is  $y_i = 4f_i(x_i/l_i - (x_i/l_i)^2)$ ;  $l_{si}$  is geometric parameter of cable in the  $i$ th span, whose expression is  $l_{si} = \int_0^{l_i} (ds/dx)^3 dx$ ;  $l_{si}$  is the equivalent longitudinal stiffness of the  $i$ th tower, whose expression is  $3E_{ti}I_{ti}/h_{ti}^3$ ;  $v_i$  is the vertical deflection of girder in the  $i$ th span;  $H_i$  is the horizontal tensile force of cable in the  $i$ th span;  $u_{hi}$  is the horizontal deflection of top node in the  $i$ th tower.

As the simplest type of TSSB, the three-tower self-anchored suspension bridge (TSSB) is taken as example in this section. We can get typical model shapes for first 2 orders vertical vibration, shown in Fig. 5 and Fig. 6.

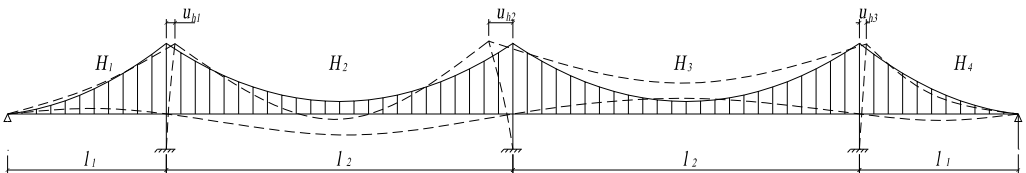


Fig. 5. Mode shape of 1st asymmetric vertical vibration

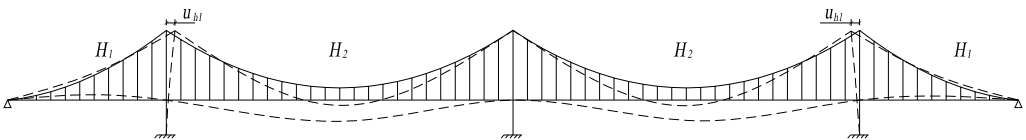


Fig. 6. Mode shape of 1st symmetric vertical vibration

Some basic assumptions are adopted in this paper containing the first 6 assumptions in reference [19]. Besides, the influence of tower stiffness to vertical vibration is considered. The deformation shapes of girder and tower for each modal are assumed based on the boundary condition and mode shape. Deformation shapes of girder are same to reference [9]. Deformation shape of tower is assumed as deformation of cantilever column under uniform lateral horizontal force. That is shown as followed:

$$u_i(x, t) = 3 \cdot \frac{u_h}{h^3} \left( \frac{1}{2} h \cdot x^2 - \frac{1}{6} \cdot x^3 \right) \cdot \sin(\omega t + \phi), \quad x \in [0, h_i], \quad i = 1, 2, 3, 4. \quad (2)$$

Based on basic assumptions, we can get vibration energy expressions of each components, such as cables, towers and girders. The expressions of kinetic energy and potential energy are deduced as followed:

$$U_{ce} = \frac{\sum_{i=1}^4 H_i^2 l_{si}}{2E_c A_c} + \frac{E_g I_{gv}}{2} \sum_{i=1}^4 \int_0^{l_i} \left( \frac{\partial^2 v}{\partial x^2} \right)^2 dx + \frac{1}{2} \sum_{i=1}^4 \int_0^{l_i} \frac{H_i^2}{E_g A_g} dx + \sum_{i=1}^3 \frac{1}{2} E_t I_{tv} \cdot \int_0^{h_i} \left( \frac{\partial^2 u_i}{\partial x^2} \right)^2 dx, \quad (3a)$$

$$T = \sum_{i=1}^4 \frac{1}{2} \int_0^{l_i} m_c \left( \frac{\partial v_i}{\partial t} \right)^2 dx + \sum_{i=1}^4 \frac{1}{2} \int_0^{l_i} m_g \left( \frac{\partial v_i}{\partial t} \right)^2 dx + \sum_{i=1}^3 \frac{1}{2} \int_0^{h_i} m_t \left( \frac{\partial u_i}{\partial t} \right)^2 dx. \quad (3b)$$

Based on force equilibrium and deformation compatibility conditions, the relations between the variables are inferred from above deflection drawing. And expressions of kinetic energy and potential energy for each component of TSSB are obtained. By the Eqs. (1), (3a), (3b), we can deduce the frequency formulas for 1st symmetric and asymmetric vertical vibration as shown in the next section. More details can refer to reference [21] (Zhangchao, 2011).

### 3.2.1. Frequency formula for 1st asymmetric vertical vibration (AVV)

Frequency of 1st symmetric vertical vibration is named  $\bar{f}_v^a$ . For symbol  $\bar{f}_v^a$ , superscript a stands for asymmetric vibration; subscript v stands for vertical vibration; the overline stands for considering the influence of tower stiffness in frequency calculation. We can get formula for frequency  $\bar{f}_v^a$  shown as followed:

$$\bar{f}_v^a = \frac{1}{2\pi} \sqrt{\frac{\alpha + \gamma_0 \cdot E_g I_g}{m_g + m_c}}, \quad (4)$$

where,  $\gamma_0$  is a variable related to lengths of each span;  $\alpha$  is a variable related to spans, ratio, tensile stiffness of cables and bending stiffness of towers, named Tower Stiffness Influence Coefficient (TSIC) for 1st AVV. Their expressions are shown as followed:

$$\gamma_0 = 97.55 / (l_1^2 l_2 + l_1^2 l_2^2 + l_1 l_2^2), \quad (5)$$

$$\alpha = 52 f_2^2 \cdot S_{t1} \cdot S_{t2} / [(l_1^3 + l_2^3)(2S_{t1} + S_{t2})]. \quad (6)$$

### 3.2.2. Frequency formula for 1st symmetric vertical vibration (SVV)

Frequency of 1st asymmetric vertical vibration is named  $\bar{f}_v^s$ . For the symbol  $\bar{f}_v^s$ , superscript s stands for asymmetric vibration; subscript v stands for vertical vibration; overline stands for considering the influence of tower stiffness in frequency calculation. We can get the calculation formula for frequency  $\bar{f}_v^s$  as followed:

$$\bar{f}_v^s = \frac{1}{2\pi} \sqrt{\frac{\beta \cdot \gamma_1 \cdot E_c A_c + \gamma_2 \cdot E_g I_{gv}}{m_g + m_c}}, \quad (7)$$

where,  $\gamma_1, \gamma_2$  are variables related to lengths of each span:

$$\gamma_1 = 2016(3l_2^2 - 4l_1^2)^2 / [(15l_1^3 l_2^4 + 95l_2^7)(l_{s1} + l_{s2})], \quad (8)$$

$$\gamma_2 = 1512(2l_2 + 3l_1)^2 / (31l_1^4 l_2 + 19l_1 l_2^4). \quad (9)$$

$\beta$  is a variable related to tensile stiffness of cables, compressive stiffness of girder and bending stiffness of towers, named Tower Stiffness Influence Coefficient (TSIC) for 1st symmetric vertical vibration. And  $B_1, B_2, B_3$  are some variables related to some structural parameters. Their expressions are shown as followed:

$$\beta = \frac{B_1^2 \cdot l_{s1} + B_1^2 \frac{E_c A_c}{E_g A_g} (l_1 + l_2) + B_2^2 \cdot l_{s2} + B_3^2 \cdot \frac{S_t}{E_c A_c}}{l_{s1} + l_{s2} + \frac{E_c A_c}{E_g A_g} (l_1 + l_2)}, \quad (10)$$

$$B_1 = \frac{-\left[3f_2 - 4f_1 \left(1 + \frac{S_t}{E_c A_c} \cdot l_{s2}\right)\right] \left[(l_{s1} + l_{s2}) + \frac{E_c A_c}{E_g A_g} (l_1 + l_2)\right]}{(3f_2 - 4f_1) \left[(l_{s1} + l_{s2}) + \frac{E_c A_c}{E_g A_g} (l_1 + l_2) + \frac{S_t}{E_c A_c} \cdot l_{s1} \cdot l_{s2} + \frac{S_t}{E_g A_g} \cdot (l_1 + l_2) \cdot l_{s2}\right]}, \quad (11a)$$

$$B_2 = \frac{-\left[3f_2 \left(1 + \frac{S_t \cdot l_{s1}}{E_c A_c} + \frac{l_1 + l_2}{E_g A_g} \cdot S_t\right) - 4f_1\right] \left[(l_{s1} + l_{s2}) + \frac{E_c A_c}{E_g A_g} (l_1 + l_2)\right]}{(3f_2 - 4f_1) \left[(l_{s1} + l_{s2}) + \frac{E_c A_c}{E_g A_g} (l_1 + l_2) + \frac{S_t}{E_c A_c} \cdot l_{s1} \cdot l_{s2} + \frac{S_t}{E_g A_g} \cdot (l_1 + l_2) \cdot l_{s2}\right]}, \quad (11b)$$

$$B_3 = \frac{-\left[3f_2 \cdot \left(l_{s1} + \frac{E_c A_c}{E_g A_g} (l_1 + l_2)\right) + 4f_1 \cdot l_{s2}\right] \left[(l_{s1} + l_{s2}) + \frac{E_c A_c}{E_g A_g} (l_1 + l_2)\right]}{(3f_2 - 4f_1) \left[(l_{s1} + l_{s2}) + \frac{E_c A_c}{E_g A_g} (l_1 + l_2) + \frac{S_t}{E_c A_c} \cdot l_{s1} \cdot l_{s2} + \frac{S_t}{E_g A_g} \cdot (l_1 + l_2) \cdot l_{s2}\right]}. \quad (11c)$$

### 3.3. Frequenceis formulas validation

#### 3.3.1. Example of physical scaled model of TSSB

The physical scaled model of TSSB in Reference [1] (Zhang C., et. al) is taken as example. A quite dense measurement location on the bridge deck in the vertical directions was proposed to identify acceptable mode shapes of the bridge in that paper. Stochastic Subspace Identification (SSI) method in the time-domain was implemented to identify the measured acceleration data. The identified most significant vertical frequencies of the TSSB scaled model bridge are summarized in that paper. Among that, frequencies of 1st asymmetric and symmetric vertical vibration are 8.16 Hz and 14.35 Hz respectively.

According to provided structural parameters in Reference [1] (Zhang C., et. al), we can get values of tower equivalent stiffness and equivalent cable length. They are shown as followed:  $S_{t1} = S_{t2} = 65.79 \text{ kN/m}$ ;  $l_{s1} = 2.05 \text{ m}$ ,  $l_{s2} = 4.15 \text{ m}$ .

Therefore, we can calculate the frequencies of first 2 vertical modals for this physical scaled TSSB model by deduced formulas in this paper.

1)  $\bar{f}_v^a$  calculated by frequency formulas:

From Eq. (5), (6), we can get  $\gamma_0 = 2.1414$ ,  $\alpha = 2.17 \times 10^{-3}$ ;

Then, according to Eq. (4), we can get  $\bar{f}_v^a = 7.9543 \text{ Hz}$ .

2)  $\bar{f}_v^s$  calculated by frequency formulas:

From Eqs. (8), (9), we can get  $\gamma_1 = 0.0253$ ;  $\gamma_2 = 3.82$ ;

From Eqs. (10), (11), we can get  $B_1 = -0.945$ ;  $B_2 = -1.031$ ;  $B_3 = -4.993$ ;  $\beta = 1.068$ ;

Then, according to Eq. (7), we can get  $\bar{f}_v^s = 13.9950 \text{ Hz}$ .

The formulas computed result and measured result are shown in Table 2. From the table, we can find that frequency computed from provided formulas are in good agreement with the result in reference [1].

**Table 2.** Frequencies comparison for two TSSB (Unit: Hz)

Modal shape	Physical scaled model of TSSB			Louzhou Bridge		
	Experiment measured	Formulas computed	Frequency difference	Experiment measured	Formulas computed	Frequency difference
1st AVV	8.1600	7.9543	-0.2057	0.4481	0.4578	0.0097
1st SVV	14.3500	13.995	-0.3550	0.6295	0.6298	0.0003

### 3.3.2. Example of practical bridge

Louzhou Bridge in section 2 is taken as an example in this part. Structural parameters of Louzhou Bridge are shown in Fig. 1. Based on modal analysis of FEM, natural frequencies of first 2 vertical mode shapes were calculated to be 0.4481 Hz and 0.6295 Hz, shown in Fig. 2 and Fig. 3.

For Louzhou Bridge, we can calculate frequencies of first 2 vertical modals, by deduced formulas in this paper, as followed.

1)  $\bar{f}_v^\alpha$  calculated by frequency formulas:

From Eqs. (5), (6), we can get  $\gamma_0 = 3.43 \times 10^{-7}$ ,  $\alpha = 9.15 \times 10^{-6}$ ;

Then, according to Eq. (4), we can get  $\bar{f}_v^\alpha = 0.4578$  (Hz).

2)  $\bar{f}_v^s$  calculated by frequency formulas:

From Eqs. (8), (9), we can get  $\gamma_1 = 1.05 \times 10^{-5}$ ;  $\gamma_2 = 6.12 \times 10^{-7}$ ;

From Eqs. (10), (11), we can get  $B_1 = -0.47$ ;  $B_2 = -1.326$ ;  $B_3 = -191.81$ ;  $\beta = 1.715$ ;

Then, according to Eq. (7), we can get  $\bar{f}_v^s = 0.6298$  (Hz).

The frequencies computed by two methods are compared in Table 2. We can come to the conclusion that the results come from deduced formulas are similar to numerical computed.

All in all, frequencies of low order vertical modal of two TSSB are calculated by deduced formulas in this paper. And the accuracy of formulas is validated by results of both experiment test data and numerical analysis result. It is a new frequency calculation method of TSSB, besides finite element method. The deduced formulas are special suitable for preliminary design stage, in which the detailed structural parameters are not sure. Through the formulas, the frequency can be estimated quickly. On the other hand, the computations of this paper can be used to test the correctness of finite element model.

## 4. Influence law of tower stiffness on frequencies

### 4.1. Influence law of tower stiffness on frequency

As we can know from above analysis, tower stiffness plays great roles in frequencies. The influence law of tower stiffness on vertical vibration will be studied in this section. Methods of formulas calculation and numerical analysis are used in this study. The structural parameters of Louzhou Bridge shown in Table 1 are taken as fundamental parameters in this section. In parameters analysis, tower stiffness is changed from 0.1 times to 1.5 times.

$\alpha$  is defined as Tower Stiffness Influence Coefficient for 1st Asymmetric Vertical Vibration (AVV). We can get changing curve of  $\alpha$  on middle tower stiffness ( $k_{tm}$ ) by Eq. (6) shown in Fig. 9. We can see from Fig. 9,  $\alpha$  increases from 1.65 to 9.15, as times of  $k_{tm}$  is changing from 0.1 to 1.0. When  $k_{tm}$  is low, value of  $\alpha$  tends to be 0.  $\alpha$  is influenced significant by stiffness of middle tower  $k_{tm}$ . In particular, gradient of  $\alpha$  become lower as times of  $k_{tm}$  enlarge. It discloses that  $\alpha$  is more sensitive to  $k_{tm}$  when  $k_{tm}$  is low.

Values of  $\bar{f}_v^\alpha$  on different  $k_{tm}$  are shown in Fig. 10. In the figure, the first line means frequencies calculated Eq. (4) proposed in this paper. The second line means frequencies analyzed

by finite element model. And the third line means frequencies calculated by Eq. in reference [9]. As we can see from the figure, frequencies calculated by Eq. (4) and “FEM”, match well in most of time, especially when the time is close to 1.  $\bar{f}_v^a$  increases from 0.3959 Hz to 0.4578 Hz as  $k_{tm}$  is changing from 2.17E+05 kN/m to 4.33E+05 kN/m. The rate of frequency increase is near 15.6%. The natural frequency  $\bar{f}_v^a$  enlarges gradually with increasing  $k_{tm}$ . The influence law of  $\bar{f}_v^a$  is similar to  $\alpha$  in Fig. 9. All in all, enlarging the value of middle tower stiffness is an effective way to improve frequency of 1st AVV.

In Fig. 10, curve of “Reference” shows as a straight line with constant value of 0.2944 Hz, as influence of tower stiffness was ignored in the formula. Comparing curves of Eq. (4) with reference [9], frequency difference is small when  $k_{tm}$  is low, while that increases as  $k_{tm}$  is enlarging. The difference shows that influence of tower stiffness cannot be ignored if  $k_{tm}$  is large. Otherwise, the error will be significant. In other words, contribution of middle tower stiffness is more and more important as tower stiffness increasing.

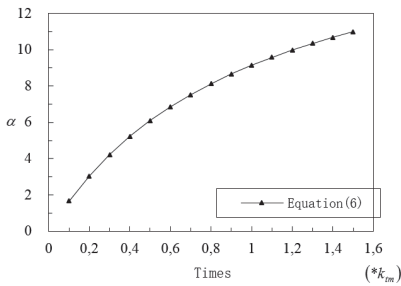


Fig. 9. Value of  $\alpha$  on different  $k_{tm}$

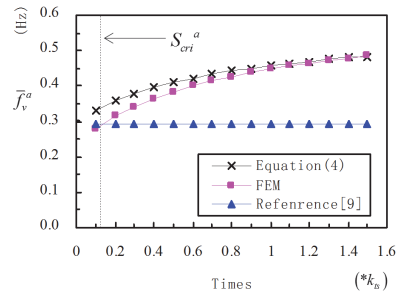


Fig. 10. Value of  $\bar{f}_v^a$  on different  $k_{tm}$

From Eq. (7), we know frequency of 1st SVV ( $\bar{f}_v^s$ ) is closely related to side tower stiffness ( $k_{ts}$ ). Therefore, we study relationship between  $\bar{f}_v^s$  and  $k_{ts}$  in following section.

$\beta$  is defined as tower Stiffness Influence Coefficient for 1st Symmetric Vertical Vibration (SVV). Based on Eq. (10), we can get curve of  $\beta$  on different side tower stiffness ( $k_{sm}$ ), as shown in Fig. 11. We can see from the figure,  $\beta$  increases as  $k_{ts}$  is enlarging. When  $k_{ts}$  is low, value of  $\beta$  tends to be 1.

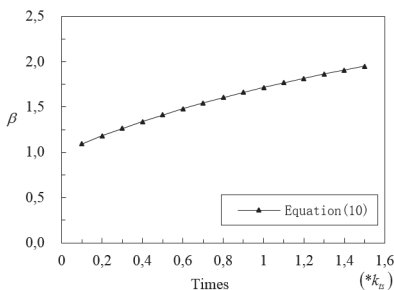


Fig. 11. Value of  $\beta$  on different  $k_{ts}$

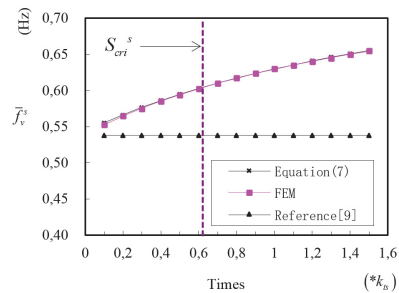


Fig. 12. Value of  $\bar{f}_v^s$  on different  $k_{ts}$

Frequencies of 1st SVV ( $\bar{f}_v^s$ ) on different  $k_{ts}$  are shown in Fig. 12. As we can see, value of  $\bar{f}_v^s$  calculated by Eq. (7) and “FEM”, match quite well. Value of  $\bar{f}_v^s$  increases from 0.5948 Hz to 0.6298 Hz as  $k_{ts}$  changing from 2.17E+05 kN/m to 4.33E+05 kN/m. The curve of  $\bar{f}_v^a$  in Fig. 12 is similar to  $\beta$  in Fig. 11.

Frequencies calculated by formula of reference [9] is shown in Fig. 12. Comparing frequencies calculated by Eq. (7) with reference [9], the values are significant different when  $k_{ts}$  is large. However, the frequencies tends to be equal when  $k_{ts}$  becomes low.

Based on the above conclusion, we can guide for the dynamic design of TSSB. Take seismic



performance design of TSSB as example, to avoid predominant period of foundation site and reduce the seismic response, long natural vibration period is expected. Based on the conclusion of this paper, lower longitudinal stiffness of middle tower is designed to reduce frequency of 1st Symmetric Vertical Vibration (SVV). At the same time, from the frequency formulas we can know that minishing mass of girder can prolong natural period too. By the same token, we can easily adjust natural period of TSSB in wind resistant design and vehicle-bridge resonance analysis.

#### 4.2. Comparing to formulas ignoring influence of tower stiffness

In Reference [19], formulas to calculate vertical frequencies were deduced neglecting influence of tower stiffness on vertical vibration, shown in Eqs. (12), (13):

$$f_v^a = \frac{1}{2\pi} \sqrt{\frac{\gamma_0 \cdot E_g I_g}{m_g + m_c}}, \tag{12}$$

$$f_v^s = \frac{1}{2\pi} \sqrt{\frac{\gamma_1 \cdot E_c A_c + \gamma_2 \cdot E_g I_{gv}}{m_g + m_c}}. \tag{13}$$

Comparing Eq. (4) and Eq. (7) to reference [9], existing of coefficient  $\alpha$  and  $\beta$  is the only difference between equations. Based on Eq. (5) and Eq. (10),  $\alpha$  and  $\beta$  are mainly related to tower stiffness. Coefficient  $\alpha$  tends to be 0 when middle tower stiffness  $k_{tm}$  is quite low. And coefficient  $\beta$  tends to be 1 when side tower stiffness  $k_{ts}$  is quite low. Therefore, when tower stiffness is quite low, Eqs. (4) and (7) can be transformed to Eq. (12) and Eq. (13) respectively. In other words, formulas in reference [9] are special forms of deduced formulas in case of low tower stiffness. Therefore, formulas in this paper are unified with that in Reference [9]. We can come to the conclusion that influence of tower stiffness on vertical vibration can be neglect when tower stiffness is low. Eqs. (12) and (13) are suggested to calculate frequency when tower stiffness is low for simplicity.

#### 4.3. Critical tower stiffness for simplified formulas

As shown in above equation,  $\bar{f}_v^s$  and  $\bar{f}_v^a$  stand for frequencies considering contribution of tower stiffness. While,  $f_v^s$  and  $f_v^a$  stand for frequencies neglecting contribution of tower stiffness.

We take formulas of  $\bar{f}_v^a$  and  $f_v^a$  as example. Obviously, the former formulas are excelling in accuracy, while the latter are simpler for calculation. The difference between  $f_v^a$  and  $\bar{f}_v^a$  comes from whether considering influence of tower stiffness. As the analysis of above section, when tower stiffness is low, the deference value would be limited. In this section, we aim to get a critical tower stiffness  $S_t^c$ . When tower stiffness below  $S_t^c$ ,  $f_v^s$  is approximately equal to  $\bar{f}_v^s$ . In this case, formulas of  $f_v^s$  can be taken to calculate low order vertical frequency more efficiently.

##### 4.3.1. Critical tower stiffness for 1st AVV

$\theta$  is defined as accuracy requirement. In general,  $\theta$  is set to be 0.9 in civil engineering. If value of  $f_v^a/\bar{f}_v^a$  is greater than  $\theta$ ,  $f_v^a$  can take place of  $\bar{f}_v^a$  in frequency evaluation. Therefore, we can get following equation:

$$\frac{f_v^a}{\bar{f}_v^a} = \sqrt{\frac{\gamma_0 \cdot E_g I_{gv}}{\alpha + \gamma_0 \cdot E_g I_{gv}}} \geq \theta. \tag{14}$$

We can assume stiffness of middle tower  $S_{tm}$  is equal to that of side tower  $S_{ts}$ . Eqs. (5) and (6)

are substituted into Eq. (14). Then the equation can transfer to following form:

$$S_{cri}^a = \frac{1.5}{\frac{8}{15} \cdot \frac{\theta^2}{1 - \theta^2} \cdot \frac{l_1 l_2 f_2^2}{(l_1 + l_2) E_g I_g} - \frac{l_{s2}}{E_c A_c}} \quad (15)$$

That is expression of critical tower stiffness for 1st AVV ( $S_{cri}^a$ ). Based on equation, we can make a judgment before calculating frequency. If  $S_{tm}$  is below to  $S_{cri}^a$ , it means the error between  $f_v^a$  and  $\bar{f}_v^a$  is limited. In this case, to simplify the calculation process, we can use Eq. (12) to evaluate frequency of 1st AVV for TSSB.

### 4.3.2. Critical tower stiffness for 1st SVV

In the same way, we can get expression of critical tower stiffness for 1st SVV ( $S_{cri}^s$ ), shown in following:

$$S_{cri}^s = \frac{(C - 1)(A + l_{s2})(3 - 4B)^2}{2(3A - 4Bl_{s2})^2 - (C - 1)Al_{s2}(3 - 4B)^2} \cdot E_c A_c, \quad (16)$$

where:  $A = l_{s1} + \frac{E_c A_c}{E_g A_g} (l_1 + l_2)$ ,  $B = \frac{l_1^2}{l_2^2}$ ,  $C = \frac{\frac{1}{\theta^2} \gamma_1 \cdot E_c A_c + (\frac{1}{\theta^2} - 1) \gamma_2 \cdot E_g I_{gv}}{\gamma_1 \cdot E_c A_c}$ .

If  $S_{ts}$  is below to  $S_{cri}^s$ , it means the error between  $f_v^s$  and  $\bar{f}_v^s$  is limited. In this case, to simplify the calculation process, we can use Eq. (13) to evaluate frequency of 1st SVV for TSSB.

We can take Louzhou Bridge in section 2 as example. Based on above Eqs. (15) and (16), we can calculate the critical tower stiffness for 1st AVV and SVV.  $\theta$  is set to be 0.9 in calculation, we can get  $S_{cri}^a$  is  $5.63 \times 10^3$  kN/m. for 1st AVV. And  $S_{cri}^s$  is  $2.68 \times 10^4$  kN/m for 1st SVV. The values are shown as dotted line in Fig. (10) and Fig. (12) respectively.

## 5. Comparing to three-tower earth-anchored suspension bridge (TESB)

Three-tower self-anchored suspension bridge (TSSB) is a special kind of bridge, which can be seen to combination of three-tower earth-anchored suspension bridge (TESB) and self-anchored suspension bridge. Therefore, it synthesizes the characters of both. In this section, structural characters of different types of bridge will be studied based on frequency formulas.

Reference [22] has deduced frequency formulas for three-tower earth-anchored suspension bridge, shown in Eqs. (17), (18):

$$f_v^a = \left(\frac{1}{2L}\right)^2 \sqrt{\frac{16\pi^2 \cdot E_g I_{gv} + \frac{(m_c + m_g)}{2f} g L^4}{(m_c + m_g)}}, \quad (17)$$

$$f_v^s = \frac{1}{2L} \sqrt{\frac{\frac{256f^2}{\pi^2 L_s L} \cdot E_c A_c + \left(\frac{\pi}{L}\right)^2 \cdot E_g I_{gv} + \frac{(m_g + m_c) g L^2}{8f}}{m_g + m_c}}, \quad (18)$$

where,  $L$ ,  $L_s$ ,  $f$  stand for span, equivalent cable length and rise respectively.

During the derivation of above formulas, influence of tower stiffness on frequencies was ignored. Therefore, to keep formulas comparable between different bridges, Eqs. (12), (13) are selected as contrastive equations.

Besides the same expressions, there are some additional expressions in frequency formulas for

MESB. In Eqs. (14), (15), there are additional expressions of  $((m_c + m_g)/2f)gL^4$  and  $(m_c + m_g)gL^2/8f$  respectively. These components mean gravity stiffness coming from dead load of cable and girder, defined as gravity stiffness component. For cable elements, stress stiffening due to great dead load of girder and cable must be considered, which is defined as effect of stress stiffening. From above formulas, we know that gravity stiffness component plays an important role in vertical stiffness of MESB. Therefore, it can significantly improve vertical frequency of MESB by increasing dead load.

However, that is different for TSSB. As cables being directly anchored to girder, girder is at compression-bending coupling state. For TSSB, effects of stress stiffening and compression-bending coupling are balanced. As a result, there is no gravity stiffness component in frequency formulas for TSSB. Therefore, increasing dead load cannot enlarge vertical stiffness of TSSB. Furthermore, it will increase seismic response of TSSB. This is one of the most significant differences between TSSB and MESB.

## 6. Conclusions

This paper is focus on frequency calculation method and influence law on frequency for TSSB. The following conclusions have been drawn from this study.

1. The finite model of first three-tower suspension bridge is established. The low order frequencies and modal shape are studied by finite element method.

2. Frequency formulas of 1st vertical AVV and SVV were deduced by Rayleigh method with considering the influence of tower stiffness. The validity of the deduced formulas is verified by results of both numerical analysis and modal test.

3. Stiffness characteristic difference between TSSB and MESB is studied by frequency formulas. The comparison discloses the significant difference is gravity stiffness component in frequency formulas.

4. Influence laws of tower stiffness on structural stiffness are studied by both formula method and finite element method. The research results show that middle tower stiffness and side tower stiffness play important role in frequency of 1st AVV and SVV respectively. Frequencies are enlarging as tower stiffness increasing. When tower stiffness is low, deduced frequency formulas are the same as formulas in other paper without considering influence of tower stiffness. At last, expressions of critical tower stiffness for simplified formulas are deduced based on deduced frequency formulas.

## Acknowledgements

The study was sponsored in part by Research Fund for the Doctoral Program Project of the Ministry of Education (No. 20133514129996) and in part by National Natural Science Foundation of Fujian Province (No. 2013J05072).

## References

- [1] Zhang C., Fang Z. Shaking table test of multi-tower self-anchored suspension bridge. *Applied Mechanics and Materials*, Vol. 353-356, 2013, p. 2216-2220.
- [2] Gimsing N. J., Georgakis C. T. *Cable supported bridges: Concept and Design*. Third edition, Wiley Online Library, 1983.
- [3] Forsberg T. Multi-span suspension bridges. *Steel Structures*, Vol. 1, Issue 1, 2001, p. 63-73.
- [4] Nazir C. P. Multispan balanced suspension bridge. *Journal of Structural Engineering*, Vol. 112, Issue 11, 1986, p. 2512-2517.
- [5] Fang Z. Z., Zhang C. Dynamic characteristics analysis and parametric study of self-anchored suspension bridge with three towers. *Journal of Earthquake Engineering and Engineering Vibration*, Vol. 36, Issue 4, 2010, p. 97-102, (in Chinese).

- [6] **Yoshida O., Okuda M., Moriya T.** Structural characteristics and applicability of Four-Span suspension bridge. *Journal of Bridge Engineering*, Vol. 9, Issue 5, 2004, p. 454-463.
- [7] **Deng Y. L., He X. J.** Seismic vulnerability analysis of long-span multi-tower suspension bridge. *International Conference on Computational and Information Science*, Chengdu, 2010, p. 458-461.
- [8] **Zhang D., Zhang Y. F.** Research on dynamic characteristics model test scheme for middle pylon of multi-pylon multi-span suspension bridges. *Engineering Sciences*, Vol. 10, Issue 3, 2012, p. 64-71.
- [9] **Jiao C. K., Li A. Q., Cao L. L., Wang H.** Traveling wave influence analysis for triple-tower suspension bridges. *China Civil Engineering Journal*, Vol. 43, Issue 12, 2010, p. 100-106, (in Chinese).
- [10] **Zhang J. W., Guo W. H., Xiang C. Q.** Dynamic characteristics analysis and parametric study of a super-long-span triple-tower suspension bridge. *Applied Mechanics and Materials*, Vol. 256-259, 2013, p. 1627-1634.
- [11] **Arzoumanidis S., Shama A., Ostadan F.** Performance-based seismic analysis and design of suspension bridges. *Earthquake Engineering and Structural Dynamics*, Vol. 34, Issue 4-5, 2005, p. 349-367.
- [12] **Au F. T. K., Cheng Y. S., Cheung Y. K.** On the determination of natural frequencies and mode shapes of cable-stayed bridges. *Applied Mathematical Modeling*, Vol. 25, 2001, p. 1099-1115.
- [13] **Jiao C. K., Li A. Q., Wang H.** Analysis on parameters of dynamic property of triple-pylon suspension bridge. *Journal of Highway and Transportation Research and Development*, Vol. 27, Issue 4, 2010, p. 51-55, (in Chinese).
- [14] **Wang L., Guo X., Noori M., Hua J.** Modal analysis of cable-tower system of twin-span suspension bridge. *Journal of Vibroengineering*, Vol. 16, Issue 4, 2014, p. 1977-1991.
- [15] **Wang H., Zou K., Li A., Jiao C. K.** Parameter effects on the dynamic characteristics of a super-long-span triple-tower suspension bridge. *Journal of Zhejiang University: Science A*, Vol. 11, Issue 5, 2010, p. 305-316.
- [16] **Wang H., Tao T., Zhou R., Hua X., Kareem A.** Parameter sensitivity study on flutter stability of a long-span triple-tower suspension bridge. *Journal of Wind Engineering and Industrial Aerodynamics*, Vol. 128, Issue 03, 2014, p. 12-21.
- [17] **Rossikhin Y. A., Shitikova M. V.** Analysis of nonlinear free vibrations of suspension bridges. *Journal of Sound and Vibration*, Vol. 186, Issue 3, 1995, p. 369-393.
- [18] **Abdel-Ghaffar A. M.** Vertical vibration analysis of suspension bridges. *Journal of the Structural Division*, Vol. 106, Issue 10, 1980, p. 2053-2075.
- [19] **Zhang C.** Simplified calculation of primary vertical frequencies for multi-tower self-anchored suspension bridge. *Journal of Wuhan University of Technology, Transportation Science and Engineering*, Vol. 37, Issue 4, 2013, p. 753-757, (in Chinese).
- [20] **Ren W. X., Peng X. L.** Baseline finite element modeling of a large span cable-stayed bridge through field ambient vibration tests. *Computers and Structures*, Vol. 83, Issue 8, 2005, p. 536-550.
- [21] **Zhang C.** Response of self-anchored suspension bridge with three-tower. Fuzhou, Fuzhou University. Doctoral dissertation, 2011, (in Chinese).
- [22] **Liu B.** Vibration characteristics research on three-tower suspension bridge. Chengdu, Southwest Jiao Tong University, Doctoral dissertation, 2009, (in Chinese).



**Chao Zhang** received the B.S. degree in Civil Engineering from Fuzhou University, China, in 2005, and his Ph.D. degree in Bridge and Tunnel Engineering from Fuzhou University, China, in 2011. Now he is an Assistant Professor in College of Civil Engineering, Fuzhou University. His research interests include seismic behavior analysis and energy dissipation of long span structure.



**Kai Huang** received the B.S. and M.S. degrees in Civil Engineering from Zhejiang University, China, in 1999 and 2002 respectively. He completed Ph.D. degrees in Civil Engineering from the Hong Kong University of Science and Technology, Hong Kong, in 2009. Now, he is an associate professor in Civil Engineering, Fuzhou University. His research interests include earthquake engineering, nonlinear structural analysis.